THE JOURNAL OF BIOLOGICAL CHEMISTRY VOL. 286, NO. 25, pp. 22456–22468, June 24, 2011
© 2011 by The American Society for Biochemistry and Molecular Biology, Inc. Printed in the U.S.A.

Differential Regulation of the Postsynaptic Clustering of γ-Aminobutyric Acid Type A ($GABA_A$) Receptors by Collybistin Isoforms*

Received for publication, March 1, 2011, and in revised form, April 21, 2011 Published, JBC Papers in Press, May 3, 2011, DOI 10.1074/jbc.M111.236190

Tzu-Ting Chiou[‡], Bevan Bonhomme[‡], Hongbing Jin[‡], Celia P. Miralles[‡], Haiyan Xiao[‡], Zhanyan Fu[§1], Robert J. Harvey[¶], Kirsten Harvey[¶], Stefano Vicini[§], and Angel L. De Blas[‡2]

From the [‡]Department of Physiology and Neurobiology, University of Connecticut, Storrs, Connecticut 06269, the [§]Department of Physiology and Biophysics, Georgetown University School of Medicine, Washington, D. C. 20057, and the [¶]Department of Pharmacology, The School of Pharmacy, London WC1N 1AX, United Kingdom

Collybistin promotes submembrane clustering of gephyrin and is essential for the postsynaptic localization of gephyrin and γ-aminobutyric acid type A ($GABA_A$) receptors at GABAergic synapses in hippocampus and amygdala. Four collybistin isoforms are expressed in brain neurons; CB2 and CB3 differ in the C terminus and occur with and without the Src homology 3 (SH3) domain. We have found that in transfected hippocampal neurons, all collybistin isoforms ($CB2_{SH3+}$, $CB2_{SH3-}$, $CB3_{SH3+}$, and $CB3_{SH3-}$) target to and concentrate at GABAergic postsynapses. Moreover, in non-transfected neurons, collybistin concentrates at GABAergic synapses. Hippocampal neurons co-transfected with $CB2_{SH3-}$ and gephyrin developed very large postsynaptic gephyrin and $GABA_A$ receptor clusters (superclusters). This effect was accompanied by a significant increase in the amplitude of miniature inhibitory postsynaptic currents. Co-transfection with $CB2_{SH3+}$ and gephyrin induced the formation of many (supernumerary) non-synaptic clusters. Transfection with gephyrin alone did not affect cluster number or size, but gephyrin potentiated the clustering effect of $CB2_{SH3-}$ or $CB2_{SH3+}$. Co-transfection with $CB2_{SH3-}$ or $CB2_{SH3+}$ and gephyrin did not affect the density of presynaptic GABAergic terminals contacting the transfected cells, indicating that collybistin is not synaptogenic. Nevertheless, the synaptic superclusters induced by $CB2_{SH3-}$ and gephyrin were accompanied by enlarged presynaptic GABAergic terminals. The enhanced clustering of gephyrin and $GABA_A$ receptors induced by collybistin isoforms was not accompanied by enhanced clustering of neuroligin 2. Moreover, during the development of GABAergic synapses, the clustering of gephyrin and $GABA_A$ receptors preceded the clustering of neuroligin 2. We propose a model in which the SH3− isoforms play a major role in the postsynaptic accumulation of $GABA_A$ receptors and in GABAergic synaptic strength.

A fundamental issue in the GABAergic synapse field is to understand the mechanisms that regulate the postsynaptic clustering of $GABA_A$[3] receptors ($GABA_A$Rs) and GABAergic synaptic strength during inhibitory synapse formation. Collybistin (CB) is a cytoplasmic protein that binds to gephyrin, helping the latter to cluster and translocate to the submembranous compartment (1–4). CB is a guanine nucleotide exchange factor (GEF) that catalyzes GDP-GTP exchange on the small GTPase Cdc42 of the Rho family (5). CB is essential for the initial synaptic localization and maintenance of gephyrin and $GABA_A$Rs at GABAergic synapses in the hippocampus and amygdala (6, 7).

In adult rat or mouse brain, two alternative spliced forms are expressed, CB2 and CB3, which are identical except for the C termini (3). There is also CB1 with a different C terminus, but this isoform is not expressed in neurons or in the adult brain. In humans, CB3 is called hPEM2. However, CB2 has not been detected in humans (3). There are also splice variants of CB2 and CB3 (or hPEM2) with or without an Src homology 3 (SH3) domain (1, 3). Although in brain and spinal cord, the mRNAs of the SH3+ are more abundant than that of SH3−, there is still a significant amount of SH3− splice forms (3). In fact, $CB2_{SH3-}$ (named Cb II by Kins *et al.* (1)) was the first CB isoform identified by a yeast two-hybrid interaction assay using a gephyrin bait (1).

All CB isoforms have a catalytic Rho guanine nucleotide exchange factor (RhoGEF) domain and a pleckstrin homology (PH) phosphoinositide-binding domain. The PH domain is essential for the translocation of gephyrin to the submembranous compartment (3) and the recruitment of gephyrin to postsynaptic sites (8, 9). However, RhoGEF activation of Cdc42 is not required for the postsynaptic clustering of gephyrin at GABAergic synapses (9).

* This work was supported, in whole or in part, by National Institutes of Health (NIH), NINDS, Grant NS38752 (to A. L. D.) and NIH, NIMH, Grant MH085224 (to Z. F.). This work was also supported by Medical Research Council Grant G0501258 (to K. H.).

[1] Present address: Dept. of Psychiatry and Behavioral Sciences, Box 3209, Duke University Medical Center, Durham, NC 27710.

[2] To whom correspondence should be addressed: Dept. of Physiology and Neurobiology, University of Connecticut, Storrs, CT 06269-3156. Tel.: 860-486-5440; Fax: 860-486-5439; E-mail: angel.deblas@uconn.edu.

[3] The abbreviations used are: $GABA_A$, γ-aminobutyric acid type A; $GABA_A$R, γ-aminobutyric acid type A receptor; mIPSC, miniature inhibitory postsynaptic current; mEPSC, miniature exitatory postsynaptic current; aa, amino acids; AMPA, α-amino-3-hydroxy-5-methyl-4-isoxazolepropionic acid; DIV, days *in vitro*; CB, collybistin; EGFP, enhanced green fluorescent protein; GAD, glutamic acid decarboxylase; HEK293 cells, human embryonic kidney 293 cells; HP, hippocampal; Ms, mouse; NL1 to -3, neuroligins 1–3, respectively; NRX, neurexin; Rb, rabbit; Ab, antibody; GEF, guanine nucleotide exchange factor; SH3, Src homology 3; PH, pleckstrin homology; NBQX, 1,2,3,4-tetrahydro-6-nitro-2,3-dioxo-benzo(*f*)quinoxaline-7-sulfonamide disodium salt hydrate.

CB SH3− isoforms are constitutively active, promoting the submembranous clustering of gephyrin (3). In contrast, the SH3+ isoforms of CB are autoinhibited by the SH3 domain. It has been shown that in HEK293 cells, neuroligin 2 (NL2) and the GABA$_A$R α2 subunit, bind to the CB SH3 domain, releasing the autoinhibition of CB (10, 11). Because NL2 is selectively localized at GABAergic synapses (12–14), it has been proposed that the postsynaptic clustering of gephyrin and GABA$_A$Rs is linked to the activation of the SH3+ isoform(s) by NL2 and/or the α2 GABA$_A$R subunit (10, 11). In contrast, little attention has been paid to the possible functional role of the SH3− isoforms. In this paper, we show that the CB SH3− isoforms play a major role in the postsynaptic accumulation of GABA$_A$Rs and GABAergic synaptic strength.

EXPERIMENTAL PROCEDURES

Animals—All of the animal protocols have been approved by the Institutional Animal Care and Use Committee of the University of Connecticut and followed the National Institutes of Health guidelines.

Antibodies—The guinea pig and rabbit (Rb) anti-rat γ2 (aa 1–15), rabbit anti-rat α1 (aa 1–15), rabbit anti-rat α2 (aa 417–423), rabbit anti-rat α3 (aa 1–13), and rabbit anti-rat α5 (aa 1–13) GABA$_A$R subunit antibodies were raised in the laboratory of Dr. De Blas against synthetic peptides. They were affinity-purified on immobilized peptide antigen. The mouse anti-β2/3 GABA$_A$R subunit mAb (clone 62-3G1) was also raised in the De Blas laboratory to the affinity-purified bovine GABA$_A$R (15, 16). It recognizes an N-terminal epitope that is common to the rat β2 and β3 subunits but not present in β1 (17). The rabbit, guinea pig, and mouse GABA$_A$R subunit antibodies have been thoroughly characterized (15, 16, 18–35). The rabbit anti-NL2 antiserum to the synthetic peptide corresponding to amino acids 750–767 of the rat NL2 was custom-made by Covance (Denver, PA). This antibody was affinity-purified on immobilized peptide antigen. In immunoblots of rat cerebral cortex, this antibody recognized a single 110,000 M_r protein band that was displaced by the immunogen peptide. In immunofluorescence of hippocampal (HP) cultures and in brain sections, the immunoreactivity specifically co-localized with that of gephyrin and γ2 GABA$_A$Rs and was apposed to GABAergic presynaptic terminals. In transfected HEK293 cells, the Ab specifically reacted with NL2 but not with NL1 or NL3. Our antibody gave an immunofluorescence signal identical to that of a different rabbit anti-NL2 antibody sample generously provided by Dr. Peter Scheiffele (Department of Cell Biology, Biozentrum, University of Basel). The mouse mAb to the SH3 domain of rat CB2 (aa 18–131) was from BD Biosciences (catalogue no. 612076, Pharmingen, San Diego, CA). The rabbit anti-CB3 antibody was raised in the laboratory of Dr. Harvey to the C terminus synthetic peptide (FWQNFSRLTPFKK) sequence that is common to rat CB3 and human hPEM2. This antibody has been previously characterized (11). The mouse monoclonal anti-gephyrin (mAb7a) was from Synaptic Systems (Gottingen, Germany; catalogue no. 147011). The sheep anti-GAD (lot no. 1440-4) was a gift from Dr. Irwin J. Kopin (NINDS, National Institutes of Health, Bethesda, MD). The Ms mAb to cMyc was from Millipore (Temecula, CA; clone 4A6, catalogue no. 05-724). Fluorophore-labeled fluorescein isothiocyanate (FITC), Texas Red, or aminomethylcoumarin species-specific anti-IgG cross-adsorbed secondary antibodies were made in donkey (Jackson ImmunoResearch Laboratories, West Grove, PA). AlexaFluor 594 or AlexaFluor 350 species-specific anti-IgG cross-adsorbed secondary antibodies (Invitrogen) were also made in donkey.

Plasmids—The rat cMyc-CB2 (SH3+ or SH3−) and rat cMyc-CB3 (SH3+ or SH3−) had the cMyc tag at the N terminus and were cloned in pRK5myc (a kind gift from Alan Hall, University College London). The hPEM2-EGFP (SH3+ or SH3−) had the enhanced green fluorescent protein (EGFP) tag at the C terminus of CB and were cloned in pEGFP-N1 (Clontech, Palo Alto, CA). The human gephyrin cDNA cloned in pcDNA3.1(+) has been described elsewhere (33). The quality of the constructs was assessed by DNA sequencing, and their expression in transfected HEK293 cells and cultured HP neurons was confirmed by immunofluorescence with antibodies (to cMyc, CB, and gephyrin) or EGFP fluorescence.

Cell Cultures—HP neuronal cultures were prepared according to Goslin *et al.* (36) as described elsewhere (21, 22, 24). Briefly, dissociated neurons from embryonic day 18 Sprague-Dawley rat hippocampi were plated at low density (3,000–8,000 cells per 18-mm diameter coverslip) for immunofluorescence or higher density (10,000–20,000 cells/18-mm diameter coverslip) for transfection and maintained in glial cell conditioned medium up to 21 days.

Immunofluorescence—Immunofluorescence of fixed HP cultures was performed as described elsewhere (21, 22, 37). Briefly, neurons grown on glass coverslips were fixed in 4% paraformaldehyde, 4% sucrose in phosphate-buffered saline (PBS) for 15 min at room temperature. The free aldehyde groups were quenched with 50 mM NH_4Cl in PBS for 10 min. Permeabilization was done with 0.25% Triton X-100 for 5 min followed by incubation with 5% normal donkey serum in 0.25% Triton X-100 in PBS for 30 min. The coverslips were incubated for 2 h at room temperature with a mixture of primary antibodies raised in different species, in the presence of 0.25% Triton X-100, followed by incubation with a mixture of species-specific secondary anti-IgG antibodies raised in donkey and conjugated to Texas Red (or AlexaFluor 594), FITC, or aminomethylcoumarin (or AlexaFluor 350) fluorophores in 0.25% Triton X-100 at room temperature for 1 h. The coverslips were washed with PBS and mounted on glass slides with Prolong Gold anti-fade mounting solution (Invitrogen).

Image Acquisition, Analysis, and Quantification—Fluorescence images of neuronal cultures were collected using a Nikon Plan Apo ×60/1.40 objective on a Nikon Eclipse T300 microscope with a Photometrics CoolSNAP HQ2 CCD camera, driven by IPLab 4.0 (Scanalytics, Rockville, MD) acquisition software. For qualitative analysis, images were processed and merged for color co-localization using Photoshop 7.0 (Adobe, San Jose, CA), adjusting brightness and contrast as described elsewhere (38). For quantification of gephyrin cluster density, two independent transfection experiments were performed for each plasmid combination. For quantification of γ2 cluster density, two independent transfections were made for each plasmid combination. All plasmid combinations were run in

each experiment. For each plasmid combination, a total of 36 dendritic fields (50 μm^2 each) from six randomly selected neurons (3 neurons/transfection, 3 dendrites/neuron, 2 dendritic fields/dendrite) were analyzed. The maximum intensities of the fluorophore channels were normalized, and the low intensity and diffuse non-clustered background fluorescence signal seen in the dendrites was subtracted. Cluster density was calculated as the number of clusters/100 μm^2 of dendritic surface. Calculated values for density (mean ± S.E.) were obtained from 148–520 gephyrin clusters and 120–387 γ2 clusters for each plasmid combination. In these low density cultures, neurons have relatively low GABAergic innervation; thus, for each plasmid combination, all of the GAD+ puncta contacting the soma and dendrites of 12 transfected neurons (from four transfection experiments, 3 neurons/transfection, randomly selected) were counted, and the density of the GAD+ presynaptic boutons was calculated as the number of GAD+ boutons contacting each neuron. Calculated values for GAD+ density was from 458–600 GAD+ puncta for each plasmid combination. For the quantification of cluster size, all of the clusters in 18 dendrites from six randomly selected neurons were analyzed (3 dendrites/neuron). GAD+ puncta size was calculated from 12 neurons. The size of gephyrin and GABA$_A$R clusters and GAD+ puncta was determined by IPLab 4.0 software. Images were segmented based on fluorescence intensity levels, to create a binary mask that maximized the number of clusters for analysis while minimizing the coalescence of individual clusters. Calculated values for size (mean ± S.E.) were obtained from 174–346 gephyrin clusters, 140–286 γ2 clusters, and 242–351 GAD+ puncta for each plasmid combination.

Cell Transfection—Cultured high density HP neurons (10 DIV) were transfected with 2 μg total of various plasmids using the CalPhos mammalian transfection kit (BD Biosciences), following the instructions of the manufacturer. Three days later after transfection, cells were subjected to immunofluorescence as described above.

Whole Cell Patch Clamp Recordings—We used an adaptation of the method described by Ortinski *et al.* (39) for cerebellar neurons. Cultured HP neurons were continuously perfused with extracellular solution, 145 mM NaCl, 5 mM KCl, 1 mM $MgCl_2$, 1 mM $CaCl_2$, 5 mM HEPES, 5 mM glucose, 15 mM sucrose, 0.25 mg/liter phenol red, and 10 μM D-serine adjusted to pH 7.4, with osmolarity of 295–305 mosM. Recording pipettes were pulled from borosilicate glass capillaries and filled with a solution containing 145 mM KCl, 10 mM HEPES, 5 mM MgATP, 0.2 mM Na_2GTP, and 5 mM EGTA, adjusted to pH 7.2 with KOH. Pipette resistance was 4–6 megaohms. Whole cell voltage clamp recordings were made at −60 mV with a PC-501A amplifier (Warner Instruments), and access resistance was monitored throughout the recordings. Currents were filtered at 1 kHz with an 8-pole low pass Bessel filter, digitized at 5–10 kHz using a computer equipped with a Digidata 1322A data acquisition board and pCLAMP9.2 software, both from Axon Instruments (Molecular Devices, Sunnyvale, CA). Spontaneous and miniature excitatory and inhibitory postsynaptic currents were identified using semiautomated threshold-based minidetection software (Mini Analysis, Synaptosoft Inc., Fort Lee, NJ) and were visually confirmed. Curve fitting and figure preparation were performed with Clampfit 9.2 software. Drugs were locally applied by means of a Y tube (40). The mIPSCs and mEPSCs were recorded in the presence of 0.5 μM tetrodotoxin and 5 μM NBQX + 1 μM strychnine (for mIPSCs) or 20 μM bicuculline (for mEPSCs). Amplitude and frequency of mIPSCs and mEPSCs of individual neurons were recorded. Values are the mean ± S.E. of 14 neurons transfected with cMyc-$CB2_{SH3-}$, gephyrin, and EGFP and 15 neurons transfected with EGFP. There were nine different transfection experiments, using the cMyc-$CB2_{SH3-}$, gephyrin, and EGFP combination and the EGFP control pairing them in each transfection experiment. The average number ± S.E. of mIPSCs recorded from each neuron was 179 ± 58 for neurons transfected with cMyc-$CB2_{SH3-}$, gephyrin, and EGFP and 125 ± 42 for neurons transfected with EGFP. The corresponding average numbers of recorded mEPSCs per neuron were 174 ± 56 and 204 ± 51, respectively.

RESULTS

Various Isoforms of Collybistin Target to and Accumulate at the GABAergic Postsynaptic Complex—We first investigated whether some or all CB isoforms expressed by neurons target to the GABAergic synapse. We transfected HP neurons with tagged $CB2_{SH3-}$, $CB2_{SH3+}$, $CB3_{SH3-}$, or $CB3_{SH3+}$. Transfection of HP neurons with hPEM2$_{SH3+}$-EGFP, which is the human orthologue of rat $CB3_{SH3+}$, showed that this EGFP-tagged CB isoform targeted to the GABAergic postsynaptic complex (Fig. 1, *A1–A4*), as shown by co-localization (*arrowheads*) with gephyrin clusters or γ2 GABA$_A$R subunit (not shown), and apposition to GAD+ presynaptic terminals. Similarly, transfection with hPEM2$_{SH3-}$-EGFP showed accumulation of EGFP fluorescence (Fig. 1, *B1* and *B2*, *arrowheads*), co-localizing with gephyrin clusters (*red*) apposed to GAD+ terminals (not shown). We have previously shown that in these cultures, gephyrin and GABA$_A$R γ2 clusters have over 90% co-localization (22).

We also checked whether the CB2 isoforms target to synapse and whether the location of the tag, using cMyc-tagged CB2 at the N terminus (cMyc-CB2) compared with the EGFP-tagged C terminus of CB3 used above (hPEM2-EGFP), affected CB synaptic targeting. Transfected neurons with cMyc-CB2 isoforms showed very strong cMyc immunofluorescence, which hampered the visualization of synaptic cMyc immunofluorescence. Nevertheless, it was clear that cMyc-$CB2_{SH3+}$ (Fig. 1*C1*) and cMyc-$CB2_{SH3-}$ (Fig. 1*D1*) accumulated (cMyc *green fluorescence*) at GABAergic synapses, as shown by apposition (*arrowheads*) to GAD+ presynaptic terminals (*blue* in Fig. 1*C2*) and co-localization (*arrowhead*) with GABA$_A$R γ2 clusters (*red* in Fig. 1*D2*) or gephyrin clusters (not shown). Fig. 1*D2* shows the presence of GABA$_A$R γ2 clusters in dendrites of both transfected (*green*) and non-transfected neurons. These results indicate that (i) $CB2_{SH3+}$, $CB2_{SH3-}$, $CB3_{SH3+}$, and $CB3_{SH3-}$ target to and concentrate at GABAergic synapses and (ii) the tagging at the N or C terminus does not affect the synaptic targeting and accumulation of the various CB isoforms.

We also investigated if endogenous CB accumulates at GABAergic synapses in non-transfected HP neurons. Triple label immunofluorescence of HP cultures using two different

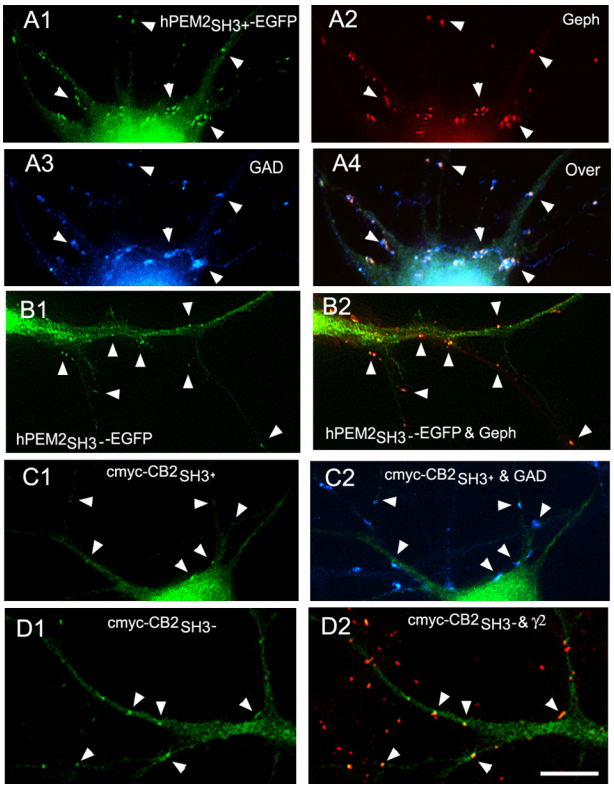

FIGURE 1. **The various tagged collybistin isoforms target to the GABAergic postsynaptic complex.** *A1–A4*, immunofluorescence of an HP neuron transfected with hPEM2$_{SH3+}$-EGFP has accumulation of EGFP fluorescence (*green*) co-localizing with gephyrin clusters (*red*) in apposition to GAD+ presynaptic terminals (*blue*). The overlay of the three fluorescence channels is shown in *A4*. The *arrowheads* indicate the presence of hPEM2$_{SH3+}$-EGFP at GABAergic synapses. *B1* and *B2*, a dendrite of a neuron transfected with hPEM2$_{SH3-}$-EGFP has accumulation of EGFP fluorescence (*green*) co-localizing with gephyrin clusters (*red*), as shown by *arrowheads*. *C1* and *C2*, the soma and dendrites of a neuron transfected with cMyc-CB2$_{SH3+}$ shows accumulation (*arrowheads*) of cMyc immunofluorescence (*green*) apposed to GAD+ presynaptic terminals (*blue*). *D1* and *D2*, the dendrites of an HP neuron transfected with cMyc-CB2$_{SH3-}$ show cMyc-CB2$_{SH3-}$ clusters (*green*) that co-localize (*arrowheads*) with GABA$_A$R γ2 clusters (*red*). The primary antibodies used were Ms mAb to gephyrin in *A2* and *B2*, sheep anti-GAD in *A3* and *C2*, Ms mAb to cMyc in *C1* and *D1*, and Rb anti-γ2 in *D2*. *Color* overlays are shown in *A4*, *B2*, *C2*, and *D2*. *Scale bar*, 10 μm for all *panels*.

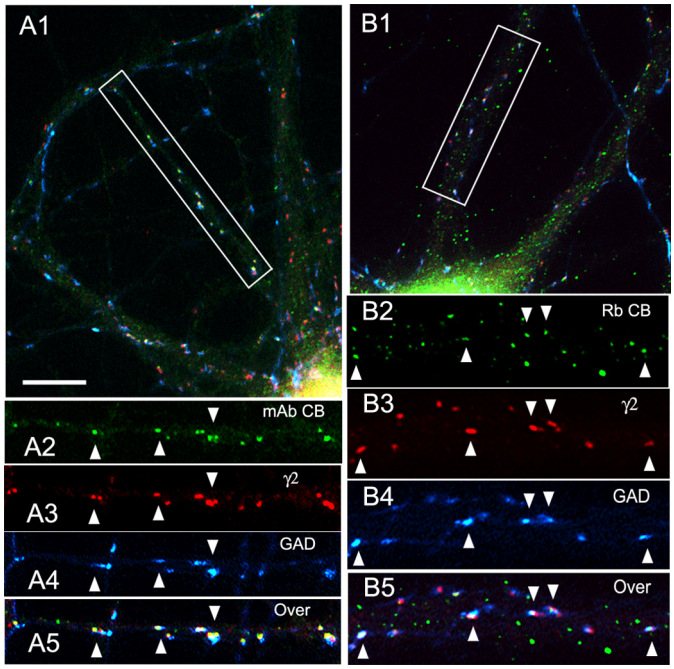

FIGURE 2. **In non-transfected hippocampal cultures, endogenous collybistin concentrates at GABAergic synapses.** *A1–A5*, triple label immunofluorescence of 21-DIV cultured HP neurons with mouse mAb to CB (*green*), Rb anti-γ2 (*red*), and sheep anti-GAD (*blue*). Overlays are shown in *A1* and *A5*. The *arrowheads* show the presence of endogenous CB immunofluorescence at GABAergic synapses. *A2–A5* correspond to the *boxed area* in A1. *B1–B5*, triple label immunofluorescence of 21-DIV cultured HP neurons with Rb anti-CB (*green*), guinea pig anti-γ2 (*red*) and sheep anti-GAD (*blue*). Overlays are shown in *B1* and *B5*. The *arrowheads* indicate the presence of endogenous CB immunofluorescence at GABAergic synapses. *B2–B5* correspond to the *boxed area* in *B1*. *Scale bar*, 10 μm in *A1* and *B1*, 9 μm in *A2–A5*, and 5.6 μm in *B2–B5*.

CB antibodies to different epitopes, the Ms anti-SH3 mAb (Fig. 2, *A1–A5*) and the rabbit anti-CB3 C terminus Ab (Fig. 2, *B1–B5*), demonstrated the presence of CB clusters (*green*) at GABAergic synapses that co-localized (*arrowheads*) with the postsynaptic GABA$_A$R γ2 subunit (*red*) and were apposed to the GAD+ presynaptic GABAergic terminals (*blue*). We have previously shown that these GAD+ and γ2 contacts correspond to synapses with actively recycling synaptic vesicles (22). There are also CB clusters not associated with GABAergic synapses or γ2 GABA$_A$R clusters (*green clusters* in Fig. 2, *A5* and *B5*, *overlays*). This is more evident for the Rb CB3 antibody. We do not know the nature of the subcellular structures associated with these non-synaptic CB3 clusters and whether they represent CB3$_{SH3-}$ isoforms. The results with two antibodies to different CB epitopes revealed the presence of CB at GABAergic synapses. To the best of our knowledge, this is the first immunocytochemical evidence that CB frequently concentrates at GABAergic synapses in non-transfected neurons.

The collybistin SH3− Isoforms Induce the Formation of Gephyrin Superclusters at GABAergic Synapses; This Effect Is Potentiated by Gephyrin—Co-transfection of HP neurons with cMyc-CB2$_{SH3-}$ and gephyrin (and EGFP) led to a dramatic increase in the size of gephyrin clusters (0.81 ± 0.03, mean ± S.E., $p < 0.001$, all in μm^2), which we call superclusters (Fig. 3, *A1* and *B1*, *red*), over sister non-transfected neurons (Fig. 3, *A2 versus A3*, *red*) or neurons transfected only with EGFP (0.24 ± 0.02). For quantification of the transfection experiments, see Fig. 6*A*. These superclusters were significantly larger than the ones resulting from transfecting the HP neurons with cMyc-CB2$_{SH3-}$ and EGFP in the absence of gephyrin (0.57 ± 0.02, $p < 0.001$), as shown in Fig. 3, *A1* and *B1 versus D*). In turn, the latter were significantly larger ($p < 0.001$) than the clusters in the control neurons transfected with EGFP (Fig. 6*A*). Thus, gephyrin potentiates the cluster size-enhancing effect of cMyc-CB2$_{SH3-}$. Interestingly, gephyrin alone (plus EGFP) did not significantly affect the size (or density; see below) of gephyrin clusters in the transfected cells over non-transfected neurons (Fig. 3*C*, *right side green neuron versus left side neuron*) or neurons transfected with EGFP. This finding is consistent with our previous observation of little or no effect of overexpressing gephyrin on gephyrin clustering (33). Note that in Fig. 3, *panels A1*, *B1*, *C*, *D*, *E*, and *F* are shown at the same magnification for cluster size comparison. It is also worth noting that cMyc-CB2$_{SH3-}$ with or without gephyrin had no significant effect on gephyrin cluster density over the EGFP controls (Fig. 6*B*).

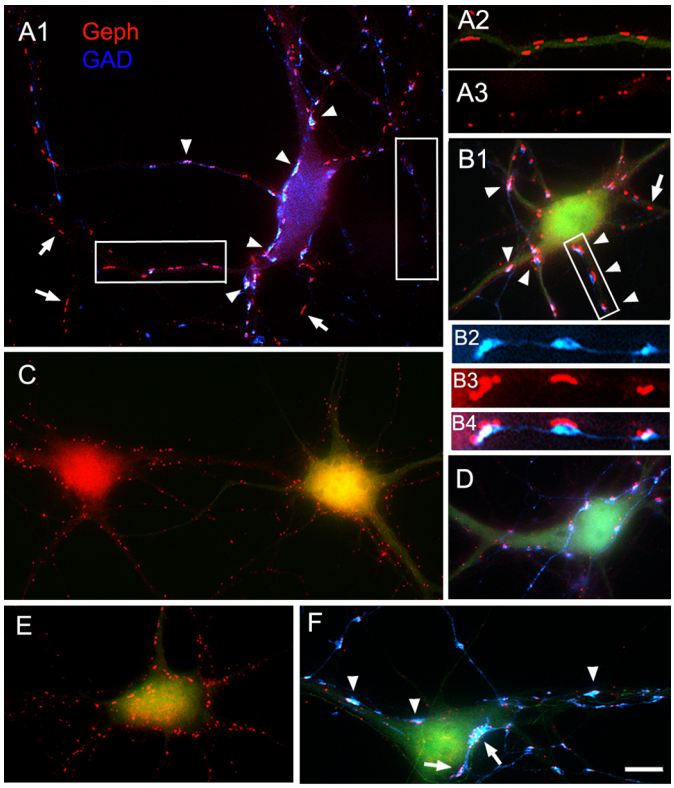

FIGURE 3. **Neurons co-transfected with cMyc-CB2$_{SH3-}$ and gephyrin develop gephyrin superclusters, frequently at GABAergic synapses.** *A1–A3* and *B1–B4*, immunofluorescence of two HP neurons co-transfected with cMyc-CB2$_{SH3-}$, gephyrin (*Geph*), and EGFP shows gephyrin superclusters (*red*) frequently apposed (*arrowheads*) to GAD+ presynaptic terminals (*blue*). Transfected cells show EGFP fluorescence (*green* in *A2* and *B1* but not shown in *A1* for better display of the *overlay* of the *blue* and *red* fluorescence channels). Compare the gephyrin cluster size in a dendrite of a transfected cell (with EGFP green fluorescence) in *A2* with that of a dendrite of a non-transfected cell (*A3*). Note the frequent apposition of GAD+ terminals to the gephyrin superclusters (*A1*, *arrowheads*, and *B2–B4*). The *arrows* in *A1* and *B1* show some superclusters with no associated presynaptic GAD+ terminal. Overlays are shown in *A1*, *A2*, *B1*, and *B4*. *A2* and *A3* correspond to *boxed areas* in *A1*. *B2–B4* correspond to the *boxed area* in *B1*. *C*, an HP neuron co-transfected with gephyrin and EGFP (no cMyc-CB3$_{SH3-}$) shows (cell on the *right* with EGFP fluorescence) that the size and density of gephyrin clusters (*red*) are not significantly different from those of a sister non-transfected neuron (neuron on the *left*). *D*, a neuron transfected with cMyc-CB2$_{SH3-}$ and EGFP (no gephyrin) has larger gephyrin clusters (*red*) than the non-transfected neurons or neurons transfected only with gephyrin (compare gephyrin cluster size in *D versus C*) but not as large as that of neurons co-transfected with cMyc-CB3$_{SH3-}$ and gephyrin (compare *D* with *A1* and *B1*). GAD immunofluorescence is shown in *blue*. *E* and *F*, two neurons transfected with cMyc-CB3$_{SH3-}$, gephyrin, and EGFP show gephyrin superclusters (*red*). The superclusters are frequently apposed (*arrows* and *arrowheads*) to GAD+ presynaptic terminals (*F*). The neuron in *F* has very large GAD+ terminals, and sometimes they are apposed to a group of smaller gephyrin clusters instead of a supercluster (*arrows*). *A1*, *B1*, and *C–F* are shown at the same magnification for cluster size comparison between neurons transfected with the various plasmid combinations. The antibodies used were Ms mAb to gephyrin and sheep anti-GAD. *Scale bar*, 10 μm in *A1*, *B1*, and *C-F*; 6.7 μm in *A2–A3*; and 4 μm in *B2–B4*.

Superclusters were present in the soma, proximal dendrites, and distal dendrites (Fig. 3*A1*, *arrows* and *arrowheads*). In some neurons, the superclusters in soma and proximal dendrites tend to be larger than the superclusters in the distal dendrites. When co-transfection with cMyc-CB2$_{SH3-}$ was made with EGFP-gephyrin (EGFP tag at the N terminus of gephyrin), instead of non-tagged gephyrin, we frequently observed the formation of EGFP-gephyrin cytoplasmic aggregates in addition to the synaptic EGFP-gephyrin clusters (not shown). Under these conditions, the superclusters tended to be absent from distal dendrites, concentrating in the soma and proximal dendrites, presumably because the formation of EGFP-gephyrin aggregates interferes with the transport of gephyrin/CB to the distal dendrites.

The gephyrin (*red*) superclusters formed after co-transfection with cMyc-CB2$_{SH3-}$ and gephyrin were frequently apposed to the blue GAD+ presynaptic terminals (Fig. 3, *A1* and *B1–B4*, *arrowheads*), indicating that many of the superclusters are associated with GABAergic synapses. Other superclusters were not apposed to GAD+ terminals (Fig. 3, *A1* and *B1*, *arrows*). The postsynaptic gephyrin superclusters frequently had a shape and orientation coinciding with that of the apposed presynaptic terminal (Fig. 3, *A1* and *B1-B4*). Quantification showed that 48.2 ± 4.9% of the gephyrin superclusters were apposed to GAD+ terminals.

We also tested whether the cMyc-CB3$_{SH3-}$ isoform induced gephyrin superclustering as cMyc-CB2$_{SH3-}$ did. Co-transfection with cMyc-CB3$_{SH3-}$, gephyrin and EGFP also led to the formation of gephyrin superclusters (*red* in Fig. 3*E*) although perhaps not as large as the superclusters obtained after transfection with cMyc-CB3$_{SH3-}$, gephyrin, and EGFP. Many of these superclusters were apposed to GAD+ (*blue*) presynaptic terminals (Fig. 3*F*, *arrows* and *arrowheads*). It is worth noting that in some synapses, instead of a postsynaptic gephyrin supercluster, a group of smaller gephyrin clusters are apposed to the GAD+ terminal (*arrows* in Fig. 3*F*).

Collybistin SH3− Induces the Formation of GABA$_A$R Superclusters at GABAergic Synapses—Co-transfection of HP neurons with cMyc-CB2$_{SH3-}$ and gephyrin also induced the superclustering of α2 GABA$_A$Rs (Fig. 4, *A1* and *A2*) and γ2 GABA$_A$Rs (Fig. 4*B*, *C1–C3*). Many of the GABA$_A$R α2 and γ2 superclusters were apposed to GAD+ presynaptic terminals (Fig. 4, *A1–A4* and *B*), indicating that these GABA$_A$R superclusters localize at GABAergic synapses. Superclusters of other GABA$_A$R subunits tested were also found, such as α1 (Fig. 4*D1*), α5 (Fig. 4*E1*), α3, and β2/3 (not shown). The GABA$_A$R superclusters co-localized with the gephyrin superclusters (Fig. 4, *C1–C3*, *D1* and *D2*, and *E1* and *E2*). Quantification showed that indeed cMyc-CB2$_{SH3-}$ (plus or minus gephyrin), induced the formation of γ2 GABA$_A$R superclusters (Fig. 6*C*) but had no effect on γ2 GABA$_A$R cluster density (Fig. 6*D*).

The Collybistin SH3+ Isoforms Induce the Formation of Non-synaptic Supernumerary Gephyrin and GABA$_A$R Clusters; This Effect Is Potentiated by Gephyrin—Co-transfection of HP neurons with the cMyc-CB2$_{SH3+}$ splice variant and gephyrin (and EGFP) led to a dramatic increase in the density (28.8 ± 4.7, $p <$ 0.001, all in number of clusters/μm^2) of gephyrin clusters (Fig. 5, *A1* and *A2*, *red*) compared with those in non-transfected neurons (Fig. 5*B*, *red*, *right cell*) or neurons transfected only with EGFP (6.1 ± 0.11). See also Fig. 6*B*. We call this phenomenon the formation of supernumerary clusters. The cluster density in neurons transfected with cMyc-CB2$_{SH3+}$ and EGFP in the absence of gephyrin (Fig. 5*B*, *left green cell*) was also significantly higher than the cluster density in control non-transfected neurons (Fig. 5*B*, *right cell*) or neurons transfected with EGFP only (20.4 ± 2.7 *versus* 6.1 ± 0.1, $p < 0.01$). The cluster density in neurons transfected with cMyc-CB2$_{SH3+}$ and

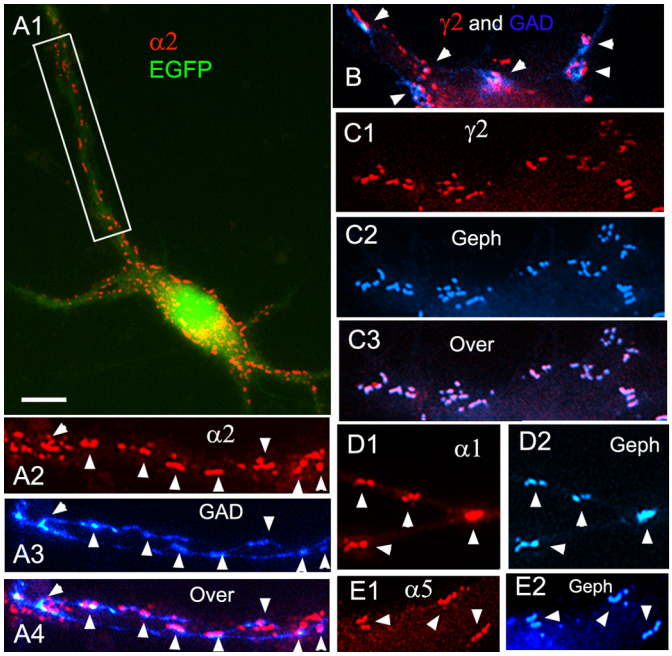

FIGURE 4. **Neurons co-transfected with cMyc-CB2$_{SH3-}$ and gephyrin develop GABA$_A$R superclusters.** *A1–A4*, immunofluorescence of a HP neuron co-transfected with cMyc-CB2$_{SH3-}$, gephyrin (*Geph*), and EGFP shows GABA$_A$R α2 superclusters (*red*) frequently apposed (*arrowheads*) to GAD+ presynaptic terminals (*blue*). *A2–A4* correspond to the *boxed areas* in *A1*. *B*, a transfected neuron shows GABA$_A$R γ2 superclusters (*red*) apposed to blue GAD+ terminals (*arrowheads*). *C1–C3*, transfected neurons show GABA$_A$R γ2 superclusters (*red*) co-localizing with the gephyrin superclusters (*blue*) as shown in the overlay (*C3*). *D1* and *D2*, dendrites of transfected neurons have GABA$_A$R α1 superclusters (*red*) co-localizing (*arrowheads*) with gephyrin superclusters (*blue*). *E1* and *E2*, dendrites of transfected cells show GABA$_A$R α5 superclusters (*red*) co-localizing (arrowheads) with gephyrin superclusters (*blue*). *Overlays* of the *red* and *blue* fluorescence are shown in *A4*, *B*, and *C3*. The EGFP fluorescence channel is not shown in the majority of the overlays to better appreciate the co-localization between the *red* and *blue* signals. *Scale bar*, 10 μm in *A1* and 4.3 μm in the other *panels*.

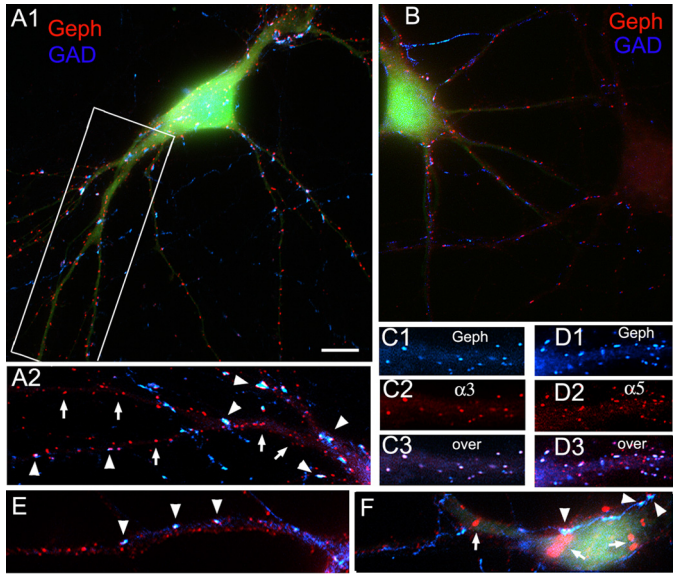

FIGURE 5. **Neurons co-transfected with cMyc-CB2$_{SH3+}$ and gephyrin develop supernumerary gephyrin and GABA$_A$R clusters, many non-synaptically localized.** *A1* and *A2*, immunofluorescence of an HP neuron co-transfected with cMyc-CB2$_{SH3+}$, gephyrin (*Geph*), and EGFP shows many gephyrin clusters (*red*). Some are apposed (*arrowheads*) to GAD+ presynaptic terminals (*blue*), but many others (*arrows*) are not. Transfected cells show EGFP fluorescence (*green*). *A1*, overlay of the three fluorescence channels; *A2*, overlay of *red* and *blue* fluorescence. *A2* corresponds to the *boxed area* in *A1*. *B*, an HP neuron transfected (neuron on the *left*) with cMyc-CB2$_{SH3+}$ and EGFP (no gephyrin) shows more gephyrin clusters than a non-transfected neuron (neuron on the *right*). *C1–C3*, in the cMyc-CB2$_{SH3+}$-, gephyrin-, and EGFP-co-transfected neurons, the majority of gephyrin clusters (*C1*, *blue*) co-localized with GABA$_A$R α3 clusters (*C2*, *red*), as shown in the overlay (*C3*). *D1–D3*, in the cMyc-CB2$_{SH3+}$-, gephyrin-, and EGFP-co-transfected neurons, many gephyrin clusters (*D1*, *blue*) co-localized with GABA$_A$R α5 clusters (*D2*, *red*) as shown in the overlay (*D3*). *E* and *F*, a dendrite (*E*) and the soma (*F*) of two neurons transfected with cMyc-CB3$_{SH3+}$, gephyrin, and EGFP. Transfected neurons normally show supernumerary gephyrin clusters (*E*), some apposed (*arrowheads*) to GAD+ terminals (*blue*). Some neurons (*F*) show large gephyrin (*red*) aggregates in the cytoplasm (*arrows*). These neurons had fewer gephyrin clusters at dendrites, but they still had GAD+ contacts (*F*, *arrowheads*). In *A2*, *C1–C3*, *D1–D3*, and *E*, the EGFP fluorescence channel is not shown to better appreciate the co-localization between the red and blue signals. The antibodies used were Ms mAb to gephyrin, sheep anti-GAD, Rb anti-α3, and Rb anti-α5. *Scale bar*, 10 μm in *A1* and *B* and 6.4 μm in *A2*, *C1–C3*, *D1–D3*, *E*, and *F*.

gephyrin (and EGFP) was higher than that of the neurons transfected with cMyc-CB2$_{SH3+}$ (and EGFP) in the absence of gephyrin (28.8 ± 4.7 *versus* 20.4 ± 2.7). This difference was not statistically significant in the analysis of variance Tukey-Kramer test ($p > 0.05$), but it was significant in the analysis of variance Student-Newman test ($p < 0.05$). Gephyrin alone had no significant effect on cluster density over the EGFP controls (Fig. 6*B*). It is also worth noting that cMyc-CB2$_{SH3+}$ with or without gephyrin did not affect cluster size over the EGFP controls as shown in Fig. 6*A*.

Co-transfection with cMyc-CB2$_{SH3+}$ and gephyrin led to the formation of supernumerary GABA$_A$R clusters containing various GABA$_A$R subunits tested, such as α3 (*red* in Fig. 5C2), α5 (*red* in Fig. 5*D2*), α1, α2, β2/3, and γ2 (not shown). These supernumerary GABA$_A$R clusters co-localized with the supernumerary gephyrin clusters (blue in Fig. 5, *C1–C3* and *D1–D3*). Quantification showed that indeed cMyc-CB2$_{SH3+}$ (plus or minus gephyrin) induced the formation of γ2 GABA$_A$R supernumerary clusters (Fig. 6*D*) but had no effect on cluster size (Fig. 6*C*). Thus, the effect of collybistin isoforms on the size or number of gephyrin clusters is accompanied by a similar effect on GABA$_A$R clusters.

Many of the supernumerary and small red gephyrin clusters formed after co-transfection with CB2$_{SH3+}$ and gephyrin were not apposed to blue GAD+ presynaptic terminals (Fig. 5, *A1* and *A2*, *arrows*), indicating that the majority of these supernumerary clusters are non-synaptic. Some of the clusters (29.6 ± 2.7%) were synaptic and apposed to GAD+ terminals (Fig. 5, *A1* and *A2*, *arrowheads*). However, a significantly higher percentage of superclusters were associated with GABAergic synapses (48.2 ± 4.9% *versus* 29.6 ± 2.7%, $p = 0.007$).

We also tested and found that the cMyc-CB3$_{SH3+}$ isoform induced supernumerary clustering, as cMyc-CB2$_{SH3+}$ did. Co-transfection with cMyc-CB3$_{SH3+}$, gephyrin, and EGFP also led to the formation of supernumerary gephyrin clusters (Fig. 5*E*). Some of these were apposed to presynaptic GAD+ terminals (*arrowheads* in Fig. 5, *E* and *F*). Nevertheless, some neurons transfected with cMyc-CB3$_{SH3+}$ and gephyrin showed very large gephyrin aggregates in the cytoplasm, which were not associated to GAD+ terminals (Fig. 5*F*, *arrows*). The neurons that had cytoplasmic aggregates had fewer gephyrin clusters at the dendrites, presumably because the aggregates prevented the normal transport of gephyrin to the dendrites. Gephyrin

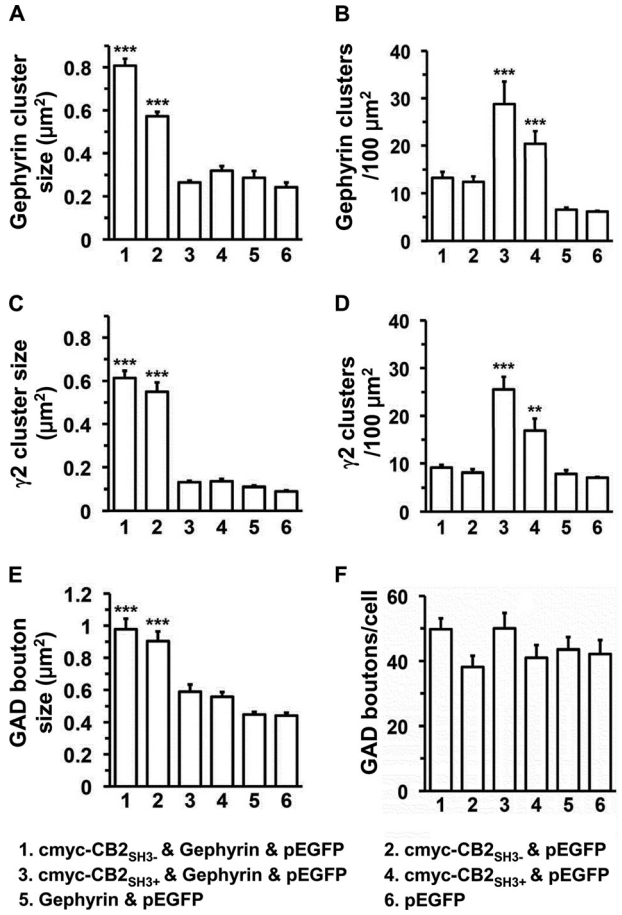

FIGURE 6. **Quantification of the effects on gephyrin and GABA$_A$R clustering and on GABAergic innervation after transfection of HP neurons with cMyc-CB2$_{SH3-}$, cMyc-CB2$_{SH3+}$, and gephyrin.** *A*, gephyrin cluster size (*1*, 0.81 ± 0.03 μm^2; *2*, 0.57 ± 0.02 μm^2; *3*, 0.26 ± 0.01 μm^2; *4*, 0.31 ± 0.02 μm^2; *5*, 0.28 ± 0.03 μm^2; *6*, 0.24 ± 0.02 μm^2). *B*, gephyrin cluster density (*1*, 13.3 ± 1.2 clusters/μm^2; *2*, 12.4 ± 1.1 clusters/μm^2; *3*, 28.8 ± 4.7 clusters/μm^2; *4*, 20.4 ± 2.7 clusters/μm^2; *5*, 6.5 ± 0.5 clusters/μm^2; *6*, 6.1 ± 0.1 clusters/100 μm^2). *C*, GABA$_A$R γ2 cluster size (*1*, 0.61 ± 0.03; *2*, 0.55 ± 0.04 μm^2; *3*, 0.13 ± 0.01 μm^2; *4*, 0.14 ± 0.01 μm^2; *5*, 0.11 ± 0.01 μm^2; *6*, 0.09 ± 0.01 μm^2). *D*, GABA$_A$R γ2 cluster density (*1*, 9.1 ± 0.6 clusters/100 μm^2; *2*, 8.1 ± 0.7 clusters/100 μm^2; *3*, 25.6 ± 2.7 clusters/100 μm^2; *4*, 16.9 ± 2.5 clusters/100 μm^2; *5*, 7.9 ± 0.7 clusters/100 μm^2; *6*, 7.1 ± 0.1 clusters/100 μm^2). *E*, GAD+ presynaptic terminal size (*1*, 0.98 ± 0.06 μm^2; *2*, 0.90 ± 0.06 μm^2; *3*, 0.59 ± 0.04 μm^2; *4*, 0.56 ± 0.03 μm^2; *5*, 0.45 ± 0.02 μm^2; *6*, 0.44 ± 0.02 μm^2). *F*, GAD+ presynaptic terminal density (*1*, 49.7 ± 3.3 GAD+ puncta/neuron; *2*, 38.2 ± 3.5 GAD+ puncta/neuron; *3*, 47.2 ± 5.4 GAD+ puncta/neuron; *4*, 41.0 ± 3.8 GAD+ puncta/neuron; *5*, 43.7 ± 3.4 GAD+ puncta/neuron; *6*, 42.8 ± 3.9 GAD+ puncta/neuron). Values are given as mean ± S.E. (*error bars*). The data were analyzed by one-way analysis of variance with a Tukey-Kramer multiple comparisons test. *Numbers 1–6* correspond to different plasmid combinations. ***, $p < 0.001$; **, $p < 0.01$ compared with *number 6* (EGFP).

aggregates were not observed in the neurons transfected with cMyc-CB2$_{SH3+}$ and gephyrin.

Neither CB2$_{SH3-}$ nor CB2$_{SH3+}$ Promote Synapse Formation; Nevertheless, CB2$_{SH3-}$ Induces Large Presynaptic GABAergic Terminals Contacting the Transfected Neurons—We also tested whether CB is synaptogenic. Quantification shows that transfection of neurons with CB2$_{SH3-}$ or CB2$_{SH3+}$ (with or without gephyrin) or just gephyrin or the EGFP-transfected controls showed no difference ($p > 0.05$) in the number (density) of presynaptic GAD+ terminals contacting the transfected neurons (Fig. 6*F*). Therefore, CB2$_{SH3+}$ and CB2$_{SH3-}$ are not synaptogenic molecules because they do not affect the number of presynaptic GABAergic boutons contacting the transfected neurons.

However, the gephyrin superclusters induced by co-transfecting cMyc-CB2$_{SH3-}$, with or without gephyrin (and EGFP), had associated large GAD+ presynaptic terminals, frequently matching the size of the postsynaptic superclusters (Fig. 3, *B2–B4*). These presynaptic terminals were significantly larger than that of control neurons transfected with EGFP as shown in Fig. 6*E*. In contrast, the size of the GAD+ terminals contacting neurons transfected with cMyc-CB2$_{SH3+}$, gephyrin, or a combination of cMyc-CB2$_{SH3+}$ and gephyrin was not significantly different from that of neurons transfected with EGFP (Fig. 6*E*).

Enlarged presynaptic GAD+ clusters were also observed in neurons transfected with cMyc-CB3$_{SH3-}$ (Fig. 3*F*, *arrows* and *arrowheads*). The neuron shown in Fig. 3*F* had particularly large presynaptic GAD+ terminals.

The GABAergic Superclusters Induced by Co-transfection with Gephyrin and CB2$_{SH3-}$ Are Accompanied by a Significant Increase in the Amplitude of mIPSCs—As indicated above, cMyc-CB2$_{SH3-}$ and gephyrin led to the formation of GABA$_A$R and gephyrin superclusters, many at GABAergic synapses (apposed to GAD+ presynaptic terminals). We tested the hypothesis that the formation of the postsynaptic GABA$_A$R superclusters had functional implications in GABAergic synapses. If that were the case, the postsynaptic superclustering of GABA$_A$Rs should be accompanied by a significant increase in the amplitude of the GABAergic mIPSCs. To test this hypothesis, we did whole cell voltage clamp recording of mIPSCs in transfected HP cultures. The amplitude of the GABAergic mIPSCs in HP neurons co-transfected with cMyc-CB2$_{SH3-}$ and gephyrin (and EGFP) was significantly higher (49 ± 5 pA, mean ± S.E., $n = 14$, $p = 0.002$) than that of the control neurons transfected with EGFP (28 ± 3 pA, $n = 15$) as shown in Fig. 7*A*. Moreover, it was relatively common for the co-transfected cells to have mIPSCs with amplitudes above 200 pA (Fig. 7*B*), which were seldom observed in control neurons (Fig. 7*C*). The cumulative probability plot (Fig. 7*D*) showed that there was a higher proportion of mIPSCs of larger amplitude in the co-transfected neurons (*red plot*) than in the controls (*black plot*). The results show that the superclusters produced by cMyc-CB2$_{SH3-}$ and gephyrin correspond to postsynaptic accumulations of functional GABA$_A$Rs.

However, there was no significant difference in the mIPSC frequency between neurons co-transfected with cMyc-CB2$_{SH3-}$ and gephyrin and control neurons transfected with EGFP (0.51 ± 0.12 *versus* 0.37 ± 0.06 Hz, $p = 0.30$) as shown in Fig. 7*A*. This result is consistent with the aforementioned immunofluorescence data showing that there was no difference in the number of GAD+ terminals contacting the neuron. Nevertheless, we have shown above that the superclustering of gephyrin and GABA$_A$Rs is accompanied by larger presynaptic GAD+ terminals. Thus, the increased size in presynaptic GAD+ terminals does not result in a significant increase in the probability of spontaneous synaptic vesicle release.

It is worth mentioning that transfection of HP neurons with gephyrin alone does not alter the amplitude or frequency of mIPSCs (41), which is consistent with our immunofluorescence

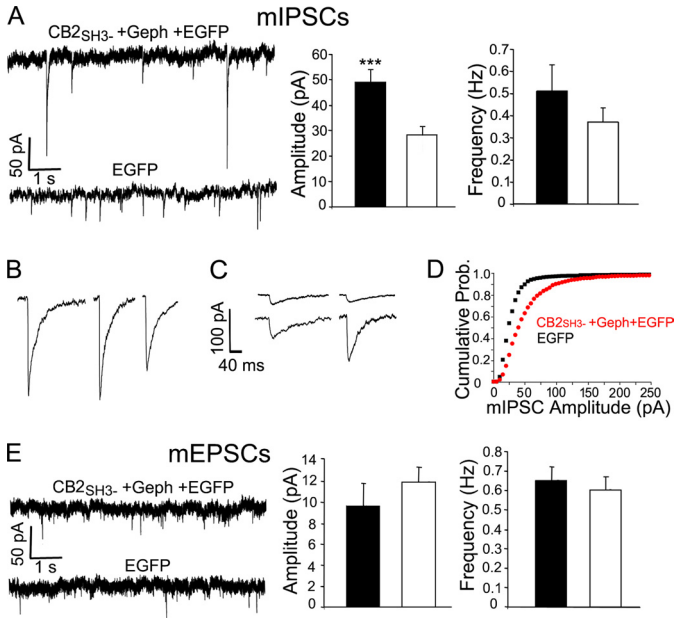

FIGURE 7. **Neurons co-transfected with cMyc-CB2$_{SH3-}$ and gephyrin show a significant increase in the amplitude of mIPSCs.** *A*, representative recordings of mIPSCs from HP neurons. The mean amplitude ± S.E. (*error bars*) of the neurons transfected with cMyc-CB2$_{SH3-}$, gephyrin (*Geph*), and EGFP (49.5 ± 5 pA, $n = 14$ neurons) was significantly larger ($p = 0.002$) in two-tailed unpaired *t* test) than that of the neurons transfected with EGFP (28 ± 3 pA, $n = 15$ neurons). There was no significant difference in the frequency (0.51 ± 0.12 *versus* 0.37 ± 0.06 Hz, $p = 0.30$). *B*, some examples of mIPSCs in neurons transfected with cMyc-CB2$_{SH3-}$, gephyrin, and EGFP. These neurons frequently showed mIPSCs of very large amplitude. *C*, some examples of mIPSCs in neurons transfected with EGFP. These neurons seldom showed mIPSCs of large amplitude. *D*, cumulative probability plots of the mIPSC amplitude of the neurons transfected with cMyc-CB2$_{SH3-}$, gephyrin, and EGFP (*red plot*) compared with that of the neurons transfected with EGFP (*black plot*). The two distributions are different ($p < 0.001$, Kolmogorov-Smirnov test). *E*, neurons transfected with cMyc-CB2$_{SH3-}$, gephyrin, and EGFP showed no significant difference in mEPSC amplitude (10 ± 2 *versus* 12 ± 2 pA, $p = 0.36$) or frequency (0.65 ± 0.07 *versus* 0.60 ± 0.06, $p = 0.57$) compared with that of neurons transfected with EGFP. Recordings were done in a voltage clamp at −60 mV in the presence of 1 mM $MgCl_2$. The mIPSCs were recorded in the presence of 0.5 μM tetrodotoxin, 5 μM NBQX, and 1 μM strychnine. The mIPSCs were blocked by 25 μM bicuculline. The mEPSCs recordings were done in the presence of 0.5 μM tetrodotoxin and 20 μM bicuculline. The mEPSCs were blocked by 5 μM NBQX. ***, $p \leq 0.002$.

results shown above indicating that gephyrin alone has no significant effect on the size or density of GABA$_A$R clusters or GAD+ presynaptic terminals. Our electrophysiology and immunofluorescence results support the notion that the GABA$_A$R superclustering induced by cMyc-CB2$_{SH3-}$ and gephyrin preferentially occurs at previously existing GABAergic synapses.

The mEPSCs of neurons transfected with cMyc-CB2$_{SH3-}$ and gephyrin (and EGFP) showed no significant difference in amplitude or frequency when compared with that of the EGFP-transfected neurons (Fig. 7*E*), indicating that the effect of CB2$_{SH3-}$ on synaptic function is specific for GABAergic synapses, having no effect on glutamatergic synapses.

The Enhanced Clustering of Gephyrin and GABA$_A$Rs Induced by Co-transfection of HP Neurons with cMyc-CB2$_{SH3-}$ or cMyc-CB2$_{SH3+}$ and Gephyrin Is Not Accompanied by Enhanced Clustering of NL2—As shown above, the co-transfection of HP neurons with cMyc-CB2$_{SH3-}$ and gephyrin induced the formation of gephyrin superclusters (*blue* in Fig. 8, *A1* and *A2*, *arrowheads*). However, this was not accompanied by the superclustering of NL2 (*red* in Fig. 8, *A1* and *A3*, *arrowheads*). Little or no accumulation of NL2 was detected in the majority of the gephyrin superclusters in the transfected cells. However, NL2 clusters co-localizing with gephyrin were present in non-transfected neurons having co-localizing gephyrin and NL2 clusters of regular size (Fig. 8, *A1–A3*, *arrows*).

As described above, the HP neurons co-transfected with cMyc-CB2$_{SH3+}$ and gephyrin showed supernumerary gephyrin clustering (*blue* in Fig. 8, *B1* and *B2*, *arrowheads*). Most if not all of the supernumerary clusters did not show NL2 co-clustering (*red* in Fig. 8, *B1* and *B3*, *arrowheads*). However, NL2 clusters co-localizing with gephyrin were present in non-transfected cells (Fig. 8, *B1–B3*, *arrows*). The presence of NL2 clusters that co-localize with gephyrin in sister non-transfected neurons served as an internal positive control for the NL2 fluorescence signal in Fig. 8, *A1–A3* and *B1–B3*.

These results indicate that (i) the superclustering or the supernumerary clustering of GABA$_A$Rs neither requires the superclustering or supernumerary clustering of endogenous NL2 nor leads to the superclustering and supernumerary co-clustering of NL2. In fact, NL2 clusters are hard to find in CB- and gephyrin-co-transfected neurons but not in EGFP-transfected or in non-transfected neurons, as shown in Figs. 8 and 9.

The Postsynaptic Accumulation of NL2 Is Delayed with Respect to the Postsynaptic Accumulation of Gephyrin and GABA$_A$Rs—We have previously shown that these low density mature HP cultures have larger postsynaptic gephyrin and GABA$_A$R clusters apposed to GAD+ terminals and smaller extrasynaptic gephyrin and GABA$_A$R clusters (22). Fig. 9, *A1–A3*, shows that in these mature (21 DIV) HP cultures, the majority of GABAergic synapses (GAD+ (*blue*) apposed to large gephyrin clusters (*red*)) have robust NL2 clusters (*green*) co-localizing with gephyrin clusters (Fig. 9, *A1–A3*, *arrowheads*) and GABA$_A$R γ2 clusters (not shown). This is in agreement with others who had previously shown that NL2 is selectively located at GABAergic postsynapses in brain and mature HP cultures (12–14). In contrast, the gephyrin clusters that are not apposed to GAD+ terminals, and some of the gephyrin clusters that are apposed to GAD terminals have no apparent NL2 associated with them (Fig. 9, *A1–A3*, *arrows*). Similarly, at 15 DIV (not shown) and at 11 DIV (Fig. 9, *B1–B3*), the majority of the GABAergic synapses have robust NL2 clusters co-localized (*arrowheads*) with gephyrin clusters in apposition to GAD+ terminals. Nevertheless, some GABAergic synapses have no NL2 clusters (*arrows*).

We have shown elsewhere that these cultures develop GAD+ presynaptic axons and synapses by 7–8 DIV (21). At 8.5 DIV, there are robust gephyrin clusters apposed to GAD+ terminals (Fig. 9, *C1–C3*, *red* and *blue*, respectively). However, at this developmental age, only few synapses showed bright, although small, NL2 clusters (*i.e.* the two NL2 clusters localized at the *right* and *left edges* of Fig. 9*C2*, *arrowheads*). The majority of the NL2 clusters were very faint and hard to distinguish from background (Fig. 9*C2*, *arrowheads*). Only their co-localization with gephyrin clusters at GABAergic synapses allowed their positive identification as NL2 clusters (as the clusters in the *middle* of Fig. 9*C2*, *arrowheads*). Therefore, although many of

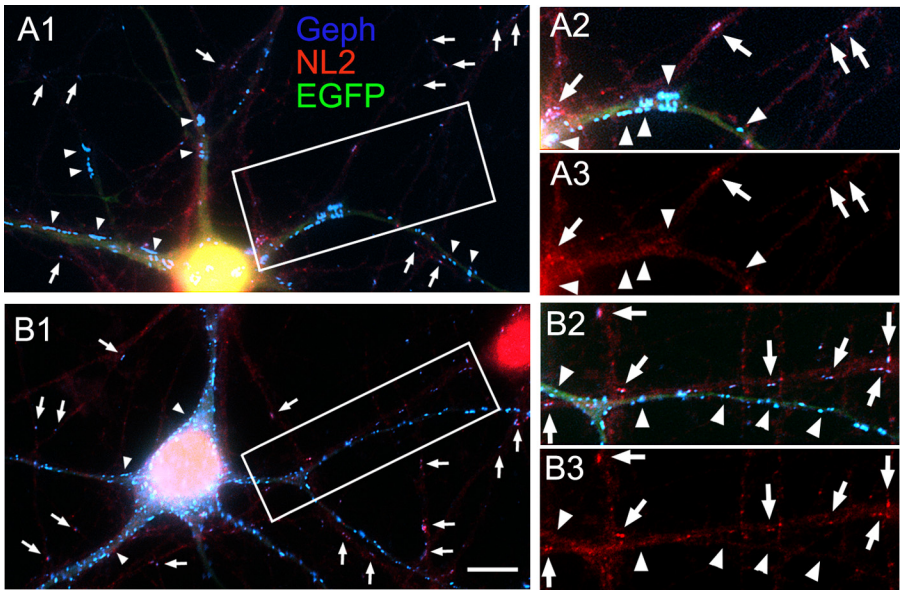

FIGURE 8. **The enhanced clustering of gephyrin and GABA$_A$Rs induced by co-transfection of HP neurons with cMyc-CB2$_{SH3-}$ or cMyc-CB2$_{SH3+}$ and gephyrin is not accompanied by enhanced clustering of NL2.** Triple label immunofluorescence is shown. *A1–A3*, an HP neuron co-transfected with cMyc-CB2$_{SH3-}$, gephyrin (*Geph*), and EGFP (*green*) has gephyrin superclusters (*blue*) but no co-localizing NL2 superclusters (*red*), as indicated by the *arrowheads*. However, regular synaptic gephyrin clusters that are present in dendrites of non-transfected neurons (*arrows*) show co-localizing NL2 clusters. *A2* and *A3* correspond to the *boxed area* in *A1*. *A1* and *A2* show the overlay of the three fluorescence channels. *B1–B3*, the supernumerary gephyrin clusters (*blue*) in a neuron co-transfected with cMyc-CB2$_{SH3+}$, gephyrin, and EGFP (*green*) show no co-localizing NL2 clusters, as indicated by *arrowheads*. However, regular synaptic gephyrin clusters in dendrites of non-transfected neurons (*arrows*) show co-localizing NL2 clusters. The *green* fluorescence allows the identification of the dendrites of transfected cells. *B2* and *B3* correspond to the *boxed area* in *B1*. *B1* and *B2* show the overlay of the three fluorescence channels. *Scale bar*, 10 μm in *A1* and *B1* and 7.3 μm in *A2*, *A3*, *B2*, and *B3*.

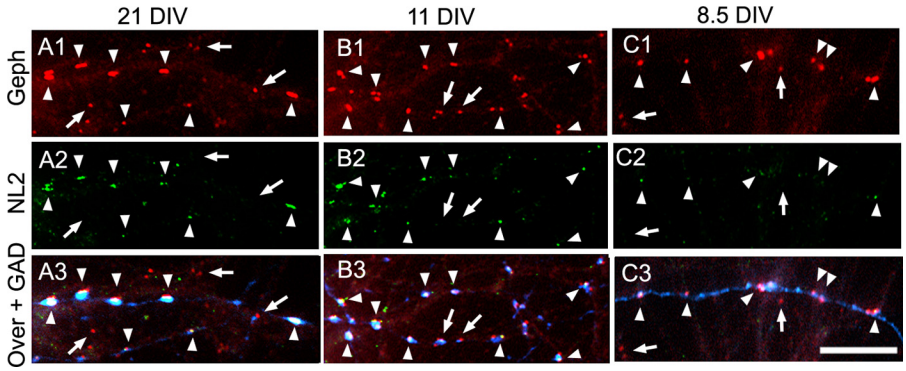

FIGURE 9. **During the development of HP cultures, the postsynaptic accumulation of NL2 is delayed with respect to the postsynaptic accumulation of gephyrin and GABA$_A$Rs.** Triple label immunofluorescence is shown. *A1–A3*, mature HP cultures (21 DIV). *B1–B3*, 11 DIV HP cultures. In 21- and 11-DIV cultures, NL2 (*green*) forms robust clusters at the majority of GABAergic synapses (*arrowheads*), co-localizing with gephyrin (*Geph*) clusters (*red*) in apposition to GAD+ terminals (*blue*). However, non-synaptic gephyrin clusters and some synaptic gephyrin clusters show no apparent NL2 co-clustering (*arrows*). *C1–C3*, at 8.5 DIV, gephyrin forms robust clusters (*red*) at GABAergic synapses (*arrowheads*) in apposition to GAD+ terminals (*blue*). However, the majority of synaptic NL2 clusters (*green*) at these synapses (*arrowheads*) are small and of low fluorescence intensity. Non-synaptic gephyrin clusters have no apparent NL2 (*arrows*). *Scale bar*, 10 μm.

the synaptic gephyrin clusters in 8.5-DIV cultures are robust with a size comparable with that of synaptic gephyrin clusters at 21 DIV (*arrowheads* in Fig. 9, *C1 versus A1*), the NL2 clusters were considerably smaller and fainter at 8.5 DIV than at 21 DIV (*arrowheads* in Fig. 9, *C2 versus A2*). At 8.5 DIV, the non-synaptic gephyrin clusters showed no NL2 (Fig. 9, *C1–C3*, *arrows*).

We have shown elsewhere that at 3.5–5.5 DIV, some neurons have some gephyrin (red) clusters that frequently co-localize with GABA$_A$R γ2 clusters (21). At these early ages, the HP cultures show no GAD immunofluorescence, indicating that the gephyrin/GABA$_A$R clusters present in the early development are not localized at GABAergic synapses (21, 42). We also tested the possible co-localization of NL2 with non-synaptic gephyrin clusters at 3.5 and 5.5 DIV. We found that at these early ages, no NL2 could be detected above background fluorescence (not shown).

Taken together, these results show that (i) during the development of the GABAergic synapses, the robust postsynaptic clustering of gephyrin and GABA$_A$Rs precedes the robust postsynaptic accumulation of NL2, and (ii) non-synaptic gephyrin and GABA$_A$R clusters have no detectable associated NL2.

DISCUSSION

Our results show that whereas the SH3− isoforms (CB2$_{SH3-}$ and CB3$_{SH3-}$) promote the gephyrin and GABA$_A$R superclustering at GABAergic synapses, the SH3+ isoforms (CB2$_{SH3+}$

and CB3$_{SH3+}$) promote the extrasynaptic supernumerary clustering of gephyrin and GABA$_A$Rs. It has been reported that overexpression in cultured HP neurons of cMyc-CB2$_{SH3+}$, cMyc-CB2$_{SH3-}$, or cMyc-hPEM2$_{SH3+}$ (the human equivalent of rat CB3) had no effect on the density or size of gephyrin clusters (3, 8), whereas overexpression cMyc-hPEM2$_{SH3-}$ caused a "modest" increase in size of gephyrin clusters (8) when compared with non-transfected neurons. Whether the studied gephyrin clusters were apposed to presynaptic GABAergic terminals or whether there was an effect on the GABAergic synaptic activity was not investigated. The apparent discrepancy with our findings could be explained because Harvey *et al.* (3) and Kalscheuer *et al.* (8) did the transfections of the HP cultures at 18 DIV and the cluster analysis at 20 or 21 DIV, whereas we did the transfections at 10 DIV and cluster analysis at 13 DIV. The effect of CB on the size and density of gephyrin clusters might be more pronounced at earlier stages of synaptic development. Their experiments were done without co-transfecting CBs with gephyrin (3, 8), which potentiates the effects of CBs, as we have shown above.

Reddy-Alla *et al.* (9) have shown that CB2$_{SH3-}$-HA, when co-transfected with gephyrin, targets to GABAergic synapses. Our findings expand on these results by showing that (i) the four CB isoforms expressed in neurons, CB2$_{SH3+}$, CB2$_{SH3-}$, hPEM2$_{SH3+}$ (CB3$_{SH3+}$), and hPEM2$_{SH3-}$ (CB3$_{SH3-}$), target to and accumulate at the GABAergic postsynaptic complex; (ii) co-transfection with gephyrin is not necessary for CB to target and accumulate at GABAergic synapses; and (iii) in non-transfected neurons, endogenous CB accumulates at GABAergic synapses.

What brings the various isoforms of CB to the GABAergic synapses? The synaptic targeting of CB is unlikely to be due to synaptic SH3 domain-binding proteins, such as NL2 and GABA$_A$R α2 subunit, because SH3− variants of CB can also target to GABAergic synapses. The synaptic targeting of CB is also unlikely to be mediated by GEF activity because mutations in the RhoGEF domain that prevent the activation of Cdc42 do not preclude the targeting of the mutant CBs to the GABAergic synapse or the normal postsynaptic clustering of gephyrin (9). However, it is noteworthy that the RhoGEF domain has a dual role in that it also interacts with gephyrin (43), suggesting that gephyrin itself could cause synaptic accumulation of CB. Last, the PH domain of CB is also essential for phosphoinositide (PI3P) interactions and clustering of CB, gephyrin, and GABA$_A$Rs (3, 8, 9), suggesting that this domain is involved in both the trafficking and synaptic targeting of CB.

It has been shown that NL2 selectively localizes at GABAergic synapses (12–14) and that NL2 binds to the SH3 domain of CB, activating it and promoting the submembranous clustering of gephyrin in COS7 and HEK293 cells (10). Poulopoulos *et al.* (10) have proposed an attractive model in which the neurexins (NRXs) of the incipient presynaptic GABAergic contacts, via trans-synaptic interaction with NL2, would induce the postsynaptic nucleation of NL2, the activation of CB SH3+ isoforms, and the postsynaptic clustering of gephyrin and GABA$_A$Rs. NL1 and NL3 do not have the CB-interacting domain; therefore, they would not promote gephyrin clustering in non-GABAergic synapses. This is consistent with the selective localization NL1 at glutamatergic synapses (44). Nevertheless, NL3 is present in some GABAergic as well as in glutamatergic synapses (45).

Although this model explains the selective accumulation of gephyrin and GABA$_A$Rs at GABAergic synapses, it does not explain several aspects of synaptic gephyrin and GABA$_A$R clustering. For example, what is the role of SH3− isoforms in the synaptic clustering of gephyrin and GABA$_A$Rs? How is that the SH3− isoforms target to GABAergic synapses and promote the postsynaptic superclustering of gephyrin and GABA$_A$Rs if these isoforms do not have the domain that interacts with synaptic NL2? How is that the overexpression of SH3+ isoforms, which interact with NL2, predominantly leads to the formation of non-synaptic supernumerary clusters?

Based on our results, we have expanded the model for the development of the GABAergic postsynaptic apparatus. The first step would be the nucleation of NL2 at synaptic contacts as an upstream mechanism for activating SH3+ isoforms and tethering gephyrin and GABA$_A$R clustering to the postsynapse, as proposed by Poulopoulos *et al.* (10). Our results indicate that the NL2 nucleation step would involve relatively few postsynaptic NL2 molecules, which would activate CB SH3+ and the formation of postsynaptic gephyrin and GABA$_A$R clusters, with no synaptic accumulation of NL2. We also propose that the SH3− isoforms are recruited to the synapse amplifying the clustering of gephyrin. There would be a simultaneous co-clustering of GABA$_A$Rs containing α2 and α3 subunits, which bind to gephyrin (11, 46). This would be an efficient feed forward control mechanism for the fast establishment of functional GABAergic synaptic contacts, in which the SH3− isoforms would play a major role. The synaptic clustering of α2 could activate CB SH3+ isoforms, further amplifying the gephyrin/GABA$_A$R clustering at synapses (11). This model requires a still unknown negative control regulatory mechanism. One possibility is the competition of some of these molecules for the binding sites on partner molecules (*i.e.* NL2 and GABA$_A$R α2 competing for the CB SH3 domain; CB and GABA$_A$R α2 competing for the overlapping binding sites on gephyrin).

It has been shown that most synaptic GABA$_A$Rs are recruited from extrasynaptic surface receptors (47, 48) and that gephyrin plays a major role in this recruiting (33, 49). The enhanced clustering of endogenous GABA$_A$Rs, induced by the overexpression of CB isoforms, indicates that there are plenty of endogenous non-clustered GABA$_A$Rs ready to be recruited to the superclusters and supernumerary clusters. Therefore, the synaptic gephyrin superclustering induced by overexpression of CB SH3− isoforms is a rate-limiting step in the postsynaptic accumulation of GABA$_A$Rs. As a rate-limiting step, it is a likely target for the regulation of the postsynaptic number of GABA$_A$Rs. We propose that the amplification of the gephyrin/GABA$_A$R clustering by CB SH3− and the regulation of the synthesis, degradation, and/or activity of the CB SH3− isoforms play a major role in determining GABAergic synaptic strength and plasticity.

It has been shown that the GABA$_A$R α2 and α3 subunits directly bind to gephyrin (11, 46). Moreover, it has been

shown that the postsynaptic clustering of GABA$_A$R α2, β2/3, and γ2 subunits is dependent on gephyrin clustering (33, 50–52). Therefore, it was not surprising that the superclustering or supernumerary clustering of gephyrin was accompanied by a similar behavior of α2, α3, γ2, and β2/3 subunits, representing the clustering of the GABA$_A$R pentamers with α2/3-β2/3-γ2 subunit composition. More surprising was the superclustering and supernumerary clustering of α1 and α5 in parallel with that of gephyrin. GABA$_A$R α1 and α5 synaptic clustering is thought to be largely independent of gephyrin (33, 51–53), and α5 is largely extrasynaptic (21, 22, 32, 54). Nevertheless, in these HP cultures, both α1 and α5 are present at GABAergic synapses (21, 22, 32, 38, 54). It is possible that CB-dependent α1 and α5 clustering is due to each of these subunits being part of a GABA$_A$R pentamer having α1 or α5 and a second α subunit that binds to gephyrin (*i.e.* α2 or α3). Alternatively, the CB-induced clustering of gephyrin might be accompanied by the co-clustering of other postsynaptic molecules directly involved in the clustering of α1 and α5 (*i.e.* radixin for α5) (55). Conceivably, the synaptic clustering of α1 and α5 could also depend on the posttranslational modification (*i.e.* phosphorylation/dephosphorylation) of GABA$_A$R subunits and/or gephyrin.

It is as yet unclear whether the SH3− isoforms are particularly involved in regulating the large size of the GABAergic perisomatic synapses and the ones at the axon initial segment (24, 54), which have stronger inhibitory drive than the smaller GABAergic synapses localized in dendrites. This notion is consistent with our aforementioned finding that the superclusters induced by the SH3− isoforms in some neurons tend to be larger in the soma than in the dendrites.

We also propose that the robust postsynaptic accumulation of NL2 is an event downstream of the robust postsynaptic clustering of gephyrin and GABA$_A$Rs. One possibility is that NL2 accumulates at GABAergic postsynapses by interacting with postsynaptic gephyrin. This is unlikely, because NL1, which also has a gephyrin-interacting domain, does not localize at GABAergic synapses; instead, NL1 accumulates at glutamatergic synapses (44). Moreover, no NL2 or other neuroligins tested (NL1 or NL3) accumulate at the gephyrin/GABA$_A$R superclusters induced by overexpression of CB2$_{SH3-}$. In addition, Papadopoulos *et al.* (6, 7) and Poulopoulos *et al.* (10) have shown that in the hippocampus of the CB KO mouse mutants, the postsynaptic clustering of gephyrin and GABA$_A$R was disrupted in soma and dendrites, whereas the postsynaptic targeting of NL2 to synapses was unaltered. Others have also shown that NL2 targets to the GABAergic synapses in the absence of postsynaptic gephyrin and GABA$_A$Rs (56). Thus, a more likely possibility is that the delayed accumulation of NL2 at GABAergic synapses results from transynaptic interaction of postsynaptic NL2 with neurexins and/or other molecules that accumulate at the presynaptic GABAergic terminals. It has been shown that neuroligins are involved in the validation of synaptically active contacts (57). The initial postsynaptic clustering of gephyrin/GABA$_A$Rs would allow the activity-dependent validation of these synapses by subsequent postsynaptic accumulation of NL2 as shown above.

The NL2 KO mouse shows selective impairment of GABAergic transmission in some brain regions but not in many others (10, 57, 58). In hippocampal pyramidal cells, perisomatic GABAergic clusters are decreased, but the postsynaptic GABAergic dendritic clusters are not affected (10). The triple KO mouse lacking NL1 to -3 shows no significant effect on gephyrin or GABAergic synaptic puncta (59). Therefore, neuroligins are dispensable for the formation of the majority of GABAergic synapses and for the postsynaptic clustering of gephyrin and GABA$_A$Rs. In contrast, gephyrin is essential for the clustering and/or anchoring of several types of GABA$_A$Rs, particularly the ones containing γ2 and α2 subunits (33, 46, 50–53). Similarly, the γ2 GABA$_A$R subunit is essential for the postsynaptic clustering of GABA$_A$Rs and gephyrin (60–63).

It has been shown that overexpression of NL2 has a synaptogenic effect promoting GABAergic innervation (14, 64), increasing the amplitude of evoked inhibitory postsynaptic currents (57) and accelerating synapse maturation (65). These effects are thought to occur via transynaptic interaction of NL2 with presynaptic NRXs (13, 66–68). Nevertheless, NLs also have neurexin-independent functions (69). In contrast, we have shown that CB overexpression of the SH3+ or SH3− isoforms is not synaptogenic because it does not affect the density of GABAergic terminals. Nevertheless, CB2$_{SH3-}$ leads to the formation of larger GAD+ presynaptic terminals matching their size to that of the postsynaptic gephyrin and GABA$_A$R superclusters. This size-matching effect reveals the existence of a transynaptic signal, probably mediated by cell adhesion molecule(s), from the postsynaptic membrane to the presynaptic terminal. This hypothetical transynaptic molecule does not seem to be postsynaptic NL2 because the enlargement of the presynaptic GAD+ terminals occurs in the absence of the postsynaptic superclustering of NL2. It could involve other postsynaptic molecules whose extracellular domains transynaptically interact with presynaptic NRXs, such as leucine-rich repeat transmembrane proteins LRRTMs (70–73), dystroglycan (74), or GABA$_A$R α1 subunit (75). It could also involve postsynaptic cell adhesion molecules that transynaptically interact with presynaptic molecules other than NRXs (for a recent review, see Ref. 76).

Acknowledgments—We thank Dr. Peter Scheiffele (Department of Cell Biology, Biozentrum, University of Basel) for a sample of Rb NL2 Ab. We thank Meng Yang for Fig. 3C.

REFERENCES

1. Kins, S., Betz, H., and Kirsch, J. (2000) *Nat. Neurosci.* **3,** 22–29
2. Rees, M. I., Harvey, K., Ward, H., White, J. H., Evans, L., Duguid, I. C., Hsu, C. C., Coleman, S. L., Miller, J., Baer, K., Waldvogel, H. J., Gibbon, F., Smart, T. G., Owen, M. J., Harvey, R. J., and Snell, R. G. (2003) *J. Biol. Chem.* **278,** 24688–24696
3. Harvey, K., Duguid, I. C., Alldred, M. J., Beatty, S. E., Ward, H., Keep, N. H., Lingenfelter, S. E., Pearce, B. R., Lundgren, J., Owen, M. J., Smart, T. G., Lüscher, B., Rees, M. I., and Harvey, R. J. (2004) *J. Neurosci.* **24,** 5816–5826
4. Fritschy, J. M., Harvey, R. J., and Schwarz, G. (2008) *Trends Neurosci.* **31,** 257–264
5. Reid, T., Bathoorn, A., Ahmadian, M. R., and Collard, J. G. (1999) *J. Biol.*

Chem. **274,** 33587–33593
6. Papadopoulos, T., Korte, M., Eulenburg, V., Kubota, H., Retiounskaia, M., Harvey, R. J., Harvey, K., O'Sullivan, G. A., Laube, B., Hülsmann, S., Geiger, J. R., and Betz, H. (2007) *EMBO J.* **26,** 3888–3899
7. Papadopoulos, T., Eulenburg, V., Reddy-Alla, S., Mansuy, I. M., Li, Y., and Betz, H. (2008) *Mol. Cell Neurosci.* **39,** 161–169
8. Kalscheuer, V. M., Musante, L., Fang, C., Hoffmann, K., Fuchs, C., Carta, E., Deas, E., Venkateswarlu, K., Menzel, C., Ullmann, R., Tommerup, N., Dalprà, L., Tzschach, A., Selicorni, A., Lüscher, B., Ropers, H. H., Harvey, K., and Harvey, R. J. (2009) *Hum. Mutat.* **30,** 61–68
9. Reddy-Alla, S., Schmitt, B., Birkenfeld, J., Eulenburg, V., Dutertre, S., Böhringer, C., Götz, M., Betz, H., and Papadopoulos, T. (2010) *Eur. J. Neurosci.* **31,** 1173–1184
10. Poulopoulos, A., Aramuni, G., Meyer, G., Soykan, T., Hoon, M., Papadopoulos, T., Zhang, M., Paarmann, I., Fuchs, C., Harvey, K., Jedlicka, P., Schwarzacher, S. W., Betz, H., Harvey, R. J., Brose, N., Zhang, W., and Varoqueaux, F. (2009) *Neuron* **63,** 628–642
11. Saiepour, L., Fuchs, C., Patrizi, A., Sassoè-Pognetto, M., Harvey, R. J., and Harvey, K. (2010) *J. Biol. Chem.* **285,** 29623–29631
12. Varoqueaux, F., Jamain, S., and Brose, N. (2004) *Eur. J. Cell Biol.* **83,** 449–456
13. Graf, E. R., Zhang, X., Jin, S. X., Linhoff, M. W., and Craig, A. M. (2004) *Cell* **119,** 1013–1026
14. Chih, B., Engelman, H., and Scheiffele, P. (2005) *Science* **307,** 1324–1328
15. De Blas, A. L., Vitorica, J., and Friedrich, P. (1988) *J. Neurosci.* **8,** 602–614
16. Vitorica, J., Park, D., Chin, G., and De Blas, A. L. (1988) *J. Neurosci.* **8,** 615–622
17. Ewert, M., De Blas, A. L., Möhler, H., and Seeburg, P. H. (1992) *Brain Res.* **569,** 57–62
18. Moreno, J. I., Piva, M. A., Miralles, C. P., and De Blas, A. L. (1994) *J. Comp. Neurol.* **350,** 260–271
19. Homanics, G. E., Harrison, N. L., Quinlan, J. J., Krasowski, M. D., Rick, C. E., De Blas, A. L., Mehta, A. K., Kist, F., Mihalek, R. M., Aul, J. J., and Firestone, L. L. (1999) *Neuropharmacology* **38,** 253–265
20. Miralles, C. P., Li, M., Mehta, A. K., Khan, Z. U., and De Blas, A. L. (1999) *J. Comp. Neurol.* **413,** 535–548
21. Christie, S. B., Li, R. W., Miralles, C. P., Riquelme, R., Yang, B. Y., Charych, E., Wendou-Yu, Daniels, S. B., Cantino, M. E., and De Blas, A. L. (2002) *Prog. Brain Res.* **136,** 157–180
22. Christie, S. B., Miralles, C. P., and De Blas, A. L. (2002) *J. Neurosci.* **22,** 684–697
23. Riquelme, R., Miralles, C. P., and De Blas, A. L. (2002) *J. Neurosci.* **22,** 10720–10730
24. Christie, S. B., and De Blas, A. L. (2003) *J. Comp. Neurol.* **456,** 361–374
25. Charych, E. I., Yu, W., Miralles, C. P., Serwanski, D. R., Li, X., Rubio, M., and De Blas, A. L. (2004) *J. Neurochem.* **90,** 173–189
26. Charych, E. I., Yu, W., Li, R., Serwanski, D. R., Miralles, C. P., Li, X., Yang, B. Y., Pinal, N., Walikonis, R., and De Blas, A. L. (2004) *J. Biol. Chem.* **279,** 38978–38990
27. Chandra, D., Korpi, E., Miralles, C. P., De Blas, A. L., and Homanics, G. E. (2005) *BMC Neurosci.* **6,** 30
28. Li, R. W., Serwanski, D. R., Miralles, C. P., Li, X., Charych, E., Riquelme, R., Huganir, R. L., and De Blas, A. L. (2005) *J. Comp. Neurol.* **488,** 11–27
29. Li, X., Serwanski, D. R., Miralles, C. P., Bahr, B. A., and De Blas, A. L. (2007) *J. Neurochem.* **102,** 1329–1345
30. Li, X., Serwanski, D. R., Miralles, C. P., Nagata, K., and De Blas, A. L. (2009) *J. Biol. Chem.* **284,** 17253–17265
31. Li, Y., Serwanski, D. R., Miralles, C. P., Fiondella, C. G., Loturco, J. J., Rubio, M. E., and De Blas, A. L. (2010) *J. Comp. Neurol.* **518,** 3439–3463
32. Serwanski, D. R., Miralles, C. P., Christie, S. B., Mehta, A. K., Li, X., and De Blas, A. L. (2006) *J. Comp. Neurol.* **499,** 458–470
33. Yu, W., Jiang, M., Miralles, C. P., Li, R. W., Chen, G., and De Blas, A. L. (2007) *Mol. Cell Neurosci.* **36,** 484–500
34. Yu, W., Charych, E. I., Serwanski, D. R., Li, R. W., Ali, R., Bahr, B. A., and De Blas, A. L. (2008) *J. Neurochem.* **105,** 2300–2314
35. Yu, W., and De Blas, A. L. (2008) *J. Neurochem.* **104,** 830–845
36. Goslin, K., Asmussen, H., and Banker, G. (1998) in *Culturing Nerve Cells*, 2nd Ed., pp. 339–370, MIT Press, Cambridge, MA
37. Christie, S. B., Li, R. W., Miralles, C. P., Yang, B. Y., and De Blas, A. L. (2006) *Mol. Cell Neurosci.* **31,** 1–14
38. Christie, S. B., and De Blas, A. L. (2002) *Neuroreport* **13,** 2355–2358
39. Ortinski, P. I., Lu, C., Takagaki, K., Fu, Z., and Vicini, S. (2004) *J. Neurophysiol.* **92,** 1718–1727
40. Murase, K., Ryu, P. D., and Randic, M. (1989) *Neurosci. Lett.* **103,** 56–63
41. Tyagarajan, S. K., Ghosh, H., Yévenes, G. E., Nikonenko, I., Ebeling, C., Schwerdel, C., Sidler, C., Zeilhofer, H. U., Gerrits, B., Muller, D., and Fritschy, J. M. (2011) *Proc. Natl. Acad. Sci. U.S.A.* **108,** 379–384
42. Studler, B., Sidler, C., and Fritschy, J. M. (2005) *J. Comp. Neurol.* **484,** 344–355
43. Xiang, S., Kim, E. Y., Connelly, J. J., Nassar, N., Kirsch, J., Winking, J., Schwarz, G., and Schindelin, H. (2006) *J. Mol. Biol.* **359,** 35–46
44. Song, J. Y., Ichtchenko, K., Südhof, T. C., and Brose, N. (1999) *Proc. Natl. Acad. Sci. U.S.A.* **96,** 1100–1105
45. Budreck, E. C., and Scheiffele, P. (2007) *Eur. J. Neurosci.* **26,** 1738–1748
46. Tretter, V., Jacob, T. C., Mukherjee, J., Fritschy, J. M., Pangalos, M. N., and Moss, S. J. (2008) *J. Neurosci.* **28,** 1356–1365
47. Thomas, P., Mortensen, M., Hosie, A. M., and Smart, T. G. (2005) *Nat. Neurosci.* **8,** 889–897
48. Bogdanov, Y., Michels, G., Armstrong-Gold, C., Haydon, P. G., Lindstrom, J., Pangalos, M., and Moss, S. J. (2006) *EMBO J.* **25,** 4381–4389
49. Jacob, T. C., Bogdanov, Y. D., Magnus, C., Saliba, R. S., Kittler, J. T., Haydon, P. G., and Moss, S. J. (2005) *J. Neurosci.* **25,** 10469–10478
50. Kneussel, M., Brandstätter, J. H., Laube, B., Stahl, S., Müller, U., and Betz, H. (1999) *J. Neurosci.* **19,** 9289–9297
51. Kneussel, M., Brandstätter, J. H., Gasnier, B., Feng, G., Sanes, J. R., and Betz, H. (2001) *Mol. Cell Neurosci.* **17,** 973–982
52. Lévi, S., Logan, S. M., Tovar, K. R., and Craig, A. M. (2004) *J. Neurosci.* **24,** 207–217
53. Fischer, F., Kneussel, M., Tintrup, H., Haverkamp, S., Rauen, T., Betz, H., and Wässle, H. (2000) *J. Comp. Neurol.* **427,** 634–648
54. Brünig, I., Scotti, E., Sidler, C., and Fritschy, J. M. (2002) *J. Comp. Neurol.* **443,** 43–55
55. Loebrich, S., Bähring, R., Katsuno, T., Tsukita, S., and Kneussel, M. (2006) *EMBO J.* **25,** 987–999
56. Patrizi, A., Scelfo, B., Viltono, L., Briatore, F., Fukaya, M., Watanabe, M., Strata, P., Varoqueaux, F., Brose, N., Fritschy, J. M., and Sassoè-Pognetto, M. (2008) *Proc. Natl. Acad. Sci. U.S.A.* **105,** 13151–13156
57. Chubykin, A. A., Atasoy, D., Etherton, M. R., Brose, N., Kavalali, E. T., Gibson, J. R., and Südhof, T. C. (2007) *Neuron* **54,** 919–931
58. Gibson, J. R., Huber, K. M., and Südhof, T. C. (2009) *J. Neurosci.* **29,** 13883–13897
59. Varoqueaux, F., Aramuni, G., Rawson, R. L., Mohrmann, R., Missler, M., Gottmann, K., Zhang, W., Südhof, T. C., and Brose, N. (2006) *Neuron* **51,** 741–754
60. Essrich, C., Lorez, M., Benson, J. A., Fritschy, J. M., and Lüscher, B. (1998) *Nat. Neurosci.* **1,** 563–571
61. Schweizer, C., Balsiger, S., Bluethmann, H., Mansuy, I. M., Fritschy, J. M., Mohler, H., and Lüscher, B. (2003) *Mol. Cell Neurosci.* **24,** 442–450
62. Alldred, M. J., Mulder-Rosi, J., Lingenfelter, S. E., Chen, G., and Lüscher, B. (2005) *J. Neurosci.* **25,** 594–603
63. Li, R. W., Yu, W., Christie, S., Miralles, C. P., Bai, J., Loturco, J. J., and De Blas, A. L. (2005) *J. Neurochem.* **95,** 756–770
64. Prange, O., Wong, T. P., Gerrow, K., Wang, Y. T., and El-Husseini, A. (2004) *Proc. Natl. Acad. Sci. U.S.A.* **101,** 13915–13920
65. Fu, Z., and Vicini, S. (2009) *Mol. Cell Neurosci.* **42,** 45–55
66. Levinson, J. N., Chéry, N., Huang, K., Wong, T. P., Gerrow, K., Kang, R., Prange, O., Wang, Y. T., and El-Husseini, A. (2005) *J. Biol. Chem.* **280,** 17312–17319
67. Craig, A. M., and Kang, Y. (2007) *Curr. Opin. Neurobiol.* **17,** 43–52
68. Südhof, T. C. (2008) *Nature* **455,** 903–911
69. Ko, J., Zhang, C., Arac, D., Boucard, A. A., Brunger, A. T., and Südhof, T. C. (2009) *EMBO J.* **28,** 3244–3255
70. Ko, J., Fuccillo, M. V., Malenka, R. C., and Südhof, T. C. (2009) *Neuron* **64,**

791–798
71. de Wit, J., Sylwestrak, E., O'Sullivan, M. L., Otto, S., Tiglio, K., Savas, J. N., Yates, J. R., 3rd, Comoletti, D., Taylor, P., and Ghosh, A. (2009) *Neuron* **64,** 799–806
72. Linhoff, M. W., Laurén, J., Cassidy, R. M., Dobie, F. A., Takahashi, H., Nygaard, H. B., Airaksinen, M. S., Strittmatter, S. M., and Craig, A. M. (2009) *Neuron* **61,** 734–749
73. Siddiqui, T. J., Pancaroglu, R., Kang, Y., Rooyakkers, A., and Craig, A. M. (2010) *J. Neurosci.* **30,** 7495–7506
74. Sugita, S., Saito, F., Tang, J., Satz, J., Campbell, K., and Südhof, T. C. (2001) *J. Cell Biol.* **154,** 435–445
75. Zhang, C., Atasoy, D., Araç, D., Yang, X., Fucillo, M. V., Robison, A. J., Ko, J., Brunger, A. T., and Südhof, T. C. (2010) *Neuron* **66,** 403–416
76. Shen, K., and Scheiffele, P. (2010) *Annu. Rev. Neurosci.* **33,** 473–507